DESIGN OF AN ION CYCLOTRON RESONANCE HEATING SYSTEM FOR THE COMPACT IGNITION TOKAMAK*

J. J. Yugo (TRW, Inc.), P. L. Goranson, D. W. Swain,
F. W. Baity, and R. Vesey (Rensselaer Polytechnic Institute)
Fusion Engineering Design Center
Oak Ridge National Laboratory
P.O. Box Y
Oak Ridge, TN 37831

Abstract

The Compact Ignition Tokamak (CIT) requires 10–20 MW of ion cyclotron resonance heating (ICRH) power to raise the plasma temperature to ignition. The initial ICRH system will provide 10 MW of power to the plasma, utilizing a total of six rf power units feeding six current straps in three ports. The system may be expanded to 20 MW with additional rf power units, antennas, and ports. Plasma heating will be achieved through coupling to the fundamental ion cyclotron resonance of a ^{3}He minority species (also the second harmonic of tritium). The proposed antenna is a resonant double loop (RDL) structure with vacuum, shorted stubs at each end for tuning and impedance matching.[1] The antennas are of modular, compact construction for installation and removal through the midplane port. Remote maintainability and the reactorlike operating environment have a major impact on the design of the launcher for this machine.

System Requirements

The ICRH system performance requirements are listed in Table 1. For the nominal operating magnetic field, the heating frequency places the ion cyclotron resonance approximately 10 cm outboard of the centerline of the plasma. This is based on experimental experience for optimal heating efficiency.[2] The tuning range of the rf sources, however, allows variation of the resonance location over a large fraction of the plasma cross section for a range of operating magnetic fields, as shown in Fig. 1. The antenna load resistance depends on the plasma density profile (and somewhat on the temperature profile) and is particularly sensitive to the density profile in the plasma scrapeoff region between the plasma edge and the antenna. Theoretical calculations give values from 1 Ω per meter of antenna length to >10 Ω/m, depending on the assumptions made about the plasma profiles. On the basis of ICRH coupling calculations and experimental measurements of antenna loading in other tokamaks, a load resistance of 2–6 Ω/m is estimated.

Table 1. Performance requirements and system overview[1,3]

Magnetic field (on axis)	10 T
Heating mode	Helium-3 minority (fundamental)
Frequency (maximum power)	95 MHz
Frequency (reduced power)	60–110 MHz
Pulse length (flattop time)	5.0 s
Power per antenna (to plasma)	1.66 MW
Assumed plasma loading	4 Ω/m
Antennas per port	Two
Total power to plasma	10 MW
Number of ports (10 MW to plasma)	Three
Time required to change frequency	4–6 h

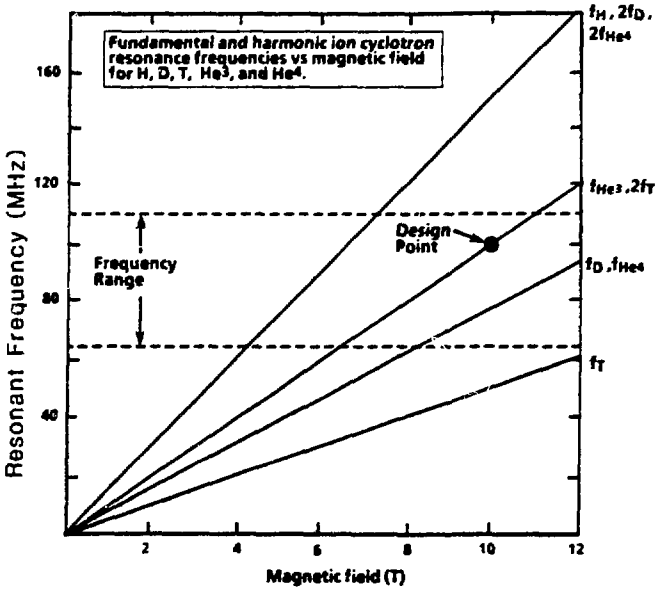

Fig. 1. Operational regime for the CIT ICRH system for different heating modes and magnetic fields.

System Overview

Antenna

The baseline antenna design consists of a pair of RDL antennas arranged poloidally in a single port (101.6 by 37.5 cm) to form one module, as shown in Figs. 2 and 3. The RDL antenna uses vacuum, shorted stubs at each end for tuning and impedance matching.[1]

Transmission Line and Impedance Matching

Radio frequency transmission is through 150 m of 9-in.-diam, 50-Ω, rigid coaxial transmission line, pressurized to 1–2 atm with dry nitrogen. The transmission line includes a 20-kV (dc) isolation section to protect the transmitters and personnel from high voltages generated during a plasma disruption. The transmission line impedance directly matches the antenna input impedance.

DC Power Supply and RF Power Units

Radio frequency power is provided by six modified surplus rf transmitter units, with Eimac X-2242 tetrodes or an improved equivalent, for an output power of 2 MW per transmitter at 95 MHz. The transmitters are located in Princeton Plasma Physics Laboratory's neutral-beam power supply building, along with rf test loads and high-power coaxial rf switches.

*Research sponsored by the Office of Fusion Energy, U.S. Department of Energy, under contract DE-AC05-84OR21400 with Martin Marietta Energy Systems, Inc.

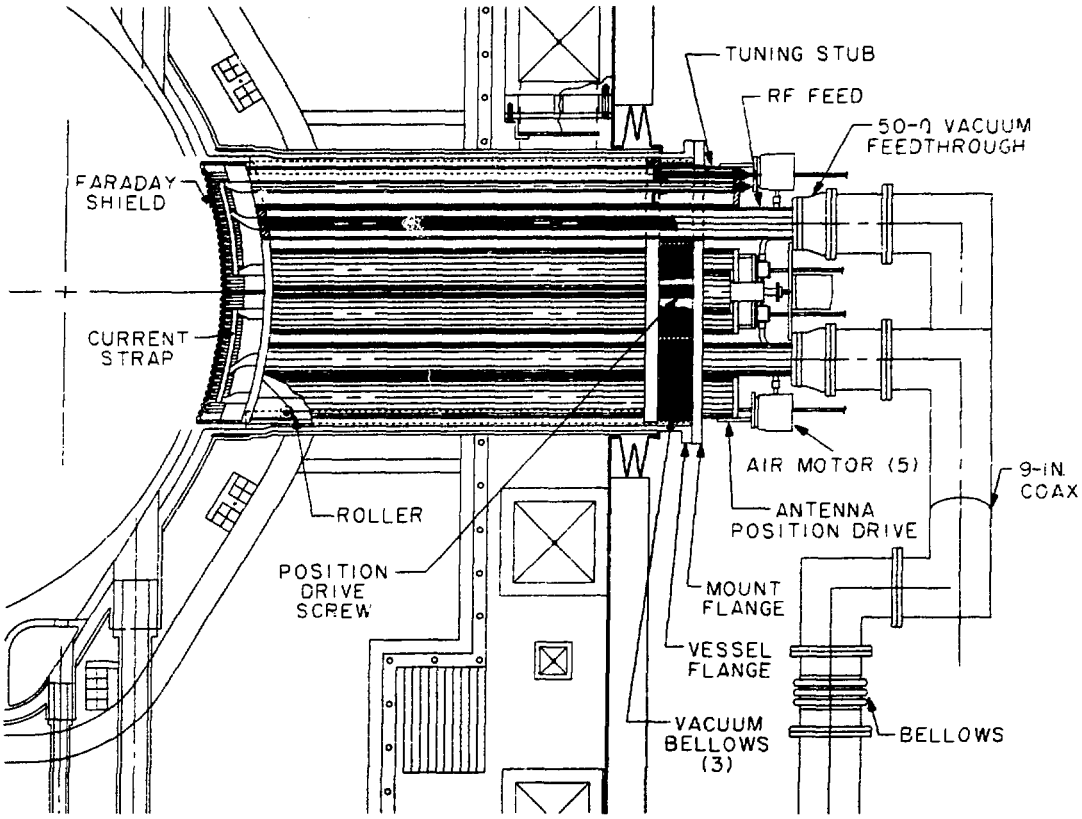

Fig. 2. Cutaway side view of the CIT antenna with major components labeled.

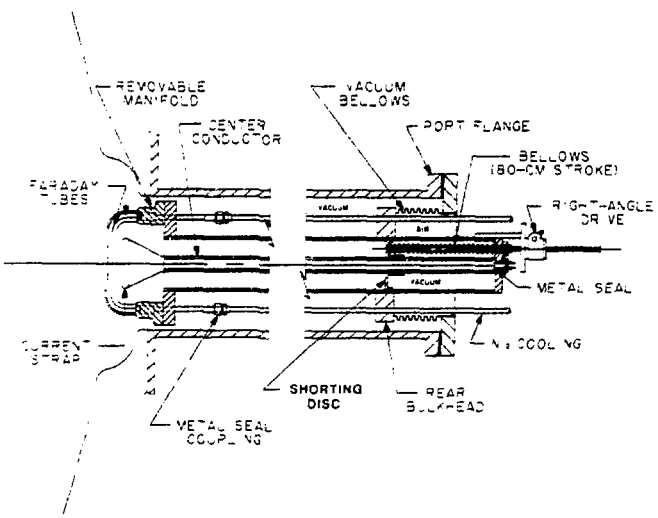

Fig. 3. Cutaway top view of the CIT antenna through one of the tuning stubs.

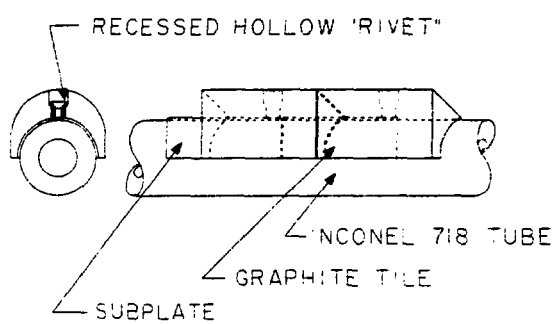

Fig. 4. Faraday shield tube section, showing one of the mechanical tile attachment possibilities.

Faraday Shield

The Faraday shield is constructed of copper-plated Inconel tubes (1/2 in. OD) in a staggered double row (Fig. 2). Graphite tiles are brazed or mechanically attached (Fig. 4) to the plasma side of the tubing. The shield is cooled with cold (100 K) nitrogen gas between shots.

Instrumentation and Control

The instrumentation and control system monitors and controls dc voltages, tuning elements (capacitors, stubs, transmitter cavities, etc.), rf power level, and pulse length. A dedicated minicomputer (micro-VAX II) with a CAMAC data acquisition system interfaces with the supervisory instrumentation and control system for safety interlocks, data transmission, and archiving. It can operate in a local, "stand-alone" mode to allow operation of the rf transmitters into test loads for system testing and tuning.

Launcher Electrical Design[1,3]

A general description of the RDL coupler is provided in Ref. 4, and relevant antenna parameters for CIT are listed in Table 2.

Table 2. Launcher design and performance parameters

Antenna input impedance	50 Ω
Tuning stub impedance	75 Ω
Peak voltage	50 kV
Peak electric field	33 kV
Maximum power per antenna (at 95 MHz)	2 MW
Maximum power per port (at 95 MHz)	4 MW
Tuning stub length range	0.6–1.4 m
Antenna tap point	0.64

A resonant circuit is formed in the RDL antenna by the combination of the antenna inductor and the two capacitive stubs at the antenna ends. A real impedance at the input to the antenna results from tapping the resonant circuit at some point along the antenna. The input impedance can be matched to the source impedance by adjusting the stubs for a given tap point as the load resistance is varied. Each end of the antenna is connected to ground through a coaxial, shorted, variable-length stub that allows tuning of the antenna to match a range of frequencies and loading impedances. Figure 5 shows the tuning stub lengths as functions of plasma load resistance for a set of baseline design parameters. For a given load resistance, an optimum tap point occurs when peak voltages at each end of the antenna are equal in magnitude. Voltages along the antenna, feedline, and tuning stubs are shown in Fig. 6 for typical operating parameters. Minimum gaps of 1.5 cm are used and occur between the ends of the antenna and the Faraday shield. The maximum power-handling capability of each antenna as a function of load resistance and frequency is plotted in Fig. 7. In this frequency range, the RDL antenna has significant advantages:

1. High-voltage, external tuning stubs are not required since the antenna input impedance is matched to the transmission line impedance.
2. Low voltage and current are maintained at the vacuum feedthrough, reducing the possibility of arcing at that point.
3. Ceramic supports, if required in the transmission line, occur where voltages are relatively low (≤15 kV at 2 MW, 50 Ω impedance).
4. Power handling by the pair of antennas is increased by up to a factor of 4 over a single antenna of the same length.

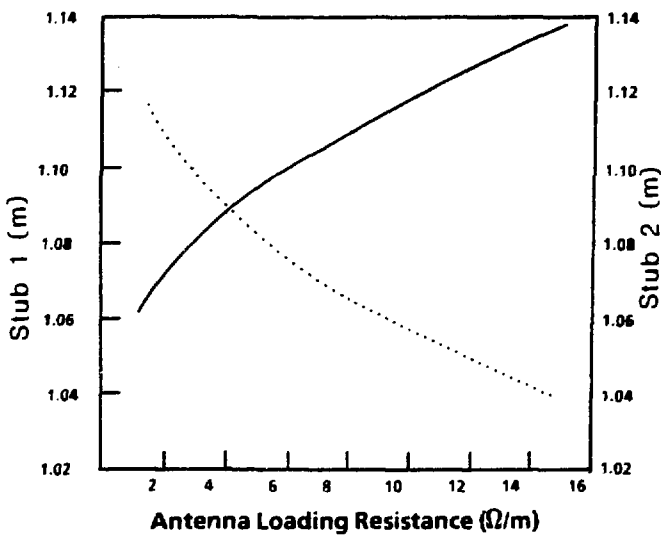

Fig. 5. Tuning stub lengths as a function of plasma loading resistance at 95 MHz for stubs having a 50-Ω impedance.

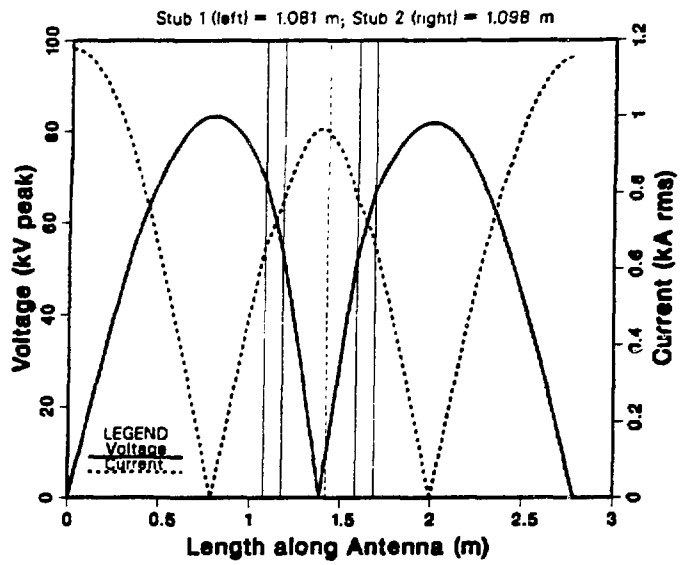

Fig. 6. Voltage and current vs distance along antenna and stub tuners at 95 MHz for a plasma loading of 4 Ω/m and V(max) = 80 kV.

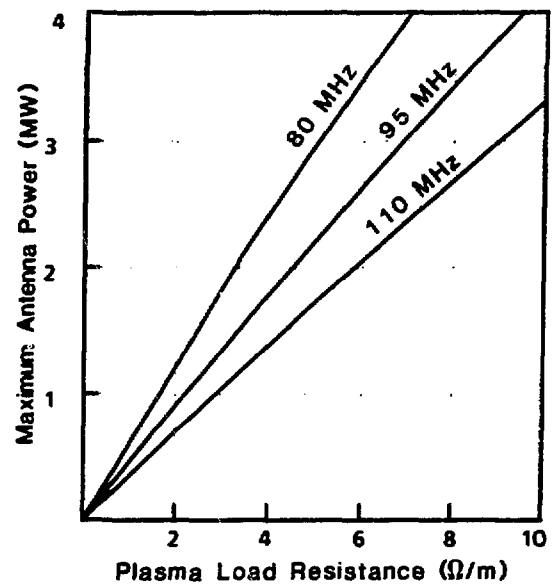

Fig. 7. Maximum antenna power vs plasma loading and frequency for V(max) = 80 kV.

Launcher Mechanical Design[1]

The antenna system interfaces with the transmission system at a constant-impedance vacuum feedthrough. The feedthrough uses a brazed-alumina dielectric to separate the pressurized 9-in. transmission line from the evacuated 4.75-in. antenna feed line. Figures 2 and 3 show the details of the side and top views of the baseline antenna configuration. The center conductor is supported by the vacuum feedthrough and by a ceramic disk in the antenna feed line. Cooling gas flows through the center conductors of the stubs to cool the antenna between shots.

The antenna elements are designed for inertial cooling during each pulse and cold gaseous nitrogen cooling between pulses

(about 1 h). The launcher module is supported by the vacuum vessel flange and port floor, which are in turn supported by the adjacent toroidal field coils. The antenna position within the port is adjusted by twin buttress-threaded shafts, capable of 140,000 lb of thrust loading. The shafts also react the vacuum and disruption loads into the vessel port flange. Tuning stub and position control shafts are both driven by air motors and rotary ball nuts, supported on thrust bearings. Vacuum bellows, metal seals, and the brazed-alumina dielectric in the feedthrough provide the vacuum boundary. A removable fixture is used to insert the launcher into, and withdraw it from, the port and to transport the module to maintenance areas remotely.

Faraday Shield Disruption Forces and Stresses[5,6]

High magnetic fields and plasma currents proposed for CIT raise concern over the design of components able to withstand the forces generated by plasma disruptions. The most critical component in the ICRH launcher, in this respect, is the Faraday shield since the shield elements form loops that intercept poloidal magnetic flux (see Fig. 3). A simplified, finite element model of the Faraday shield was used to determine the forces caused by a stationary plasma disruption.[5] The forces resulting from the disruption modeling were then used in two-dimensional (2-D) and three-dimensional (3-D) thermal and stress models to determine the total stresses in the Faraday shield tubes from plasma disruption, plasma particle flux, neutron flux, plasma radiation, and rf losses.[6] This analysis was carried out for four candidate materials: Inconel 718; TZM (Mo); Ta–10W; and Cu). The four materials analyzed represented a wide range of electrical and mechanical material properties. Table 3 summarizes the results of 2-D thermal stress calculations and 3-D disruption force and stress calculations on the Faraday shield tubes. Four candidate tube materials were analyzed with brazed graphite tiles and one with mechanically attached tiles. Three-dimensional stress analysis using combined thermal and disruption loads is incomplete but cannot yield lower values than those quoted from the present analysis.

For the disruption and heat loads used in this analysis, the only material that survives with brazed graphite tiles (marginally) is the alloy Ta–10W. Clearly, a more detailed analysis is warranted, and refinement of the incident heat loads is essential. Mechanical attachment of the graphite tiles, however, offers to eliminate the major source of stress (thermal) in the Faraday shield tubes.

Mechanically Attached Graphite Tile Design

The option for attaching graphite tiles to the Faraday shield mechanically appears desirable, given the preliminary thermal and stress data for brazed-tile cases. Mechanical attachment thermally decouples the tile from the tube, and heat transfer becomes primarily radiation. In this case, the graphite tile becomes much hotter than the equivalent brazed-tile case (700°C), and the tube remains much cooler (~123°C). With the braze eliminated, the assembly can be operated at the temperature limits for the tube (630°C) and the tile (2000°C).

Figure 4 shows one potential method of attaching graphite tiles mechanically. The tile is held to the tube by a recessed pin, wire staple, or rivet, which is welded to the tube. The rivets can be welded directly to the Faraday shield tubes or to an intermediate metal subplate, which is then spot-welded to the tube. The mounting holes are plugged with graphite rod after assembly. Both assembly options simplify the fabrication and assembly of Faraday shield tubes and tiles since individual tile braze failures no longer cause rejection of entire Faraday shield tubes or assemblies.

For the level of heat loads projected in CIT and similar machines, material choices become very limited, especially when the material must also withstand substantial mechanical loading. Separating the functions of thermal shielding and mechanical strength by thermally isolating the graphite tiles from the Faraday shield tubes appears to be an attractive alternative.

Mechanically attached tiles offer the potential of repairability, lower failure risk during assembly, and improved operational performance.

References

[1] Compact Ignition Tokamak Systems Description Document, Rev. 1, Princeton Plasma Physics Laboratory, October 1987.

[2] P. Colestock, Princeton Plasma Physics Laboratory, private communication.

[3] Compact Ignition Tokamak Conceptual Design Report, Princeton Plasma Physics Laboratory, June 6, 1986.

[4] T. L. Owens, F. W. Baity, and D. J. Hoffman, "ICRF Antenna and Feedthrough Development at the Oak Ridge National Laboratory," *Proceedings of the Sixth Topical Conference on Radio Frequency Plasma Heating, Calloway Gardens, Georgia*, American Institute of Physics Conference Proceedings No. 129, pp. 95–98, 1985.

[5] J. Bialek, Princeton Plasma Physics Laboratory, private communication, June 18, 1987.

[6] R. A. Vesey, "Thermal and Mechanical Analysis of the Faraday Shield for the Compact Ignition Tokamak," Oak Ridge National Laboratory Report ORNL/FEDC-87/5 (to be published).

Table 3. Summary of Faraday shield tube stresses for four candidate materials[6]

Faraday shield tube material	Peak (2-D) thermal stress intensity (MPa)	Thermal stress allowable (MPa)[a]	Peak (3-D) disruption stress intensity (MPa)	Disruption stress allowable (MPa)[b]	Graphite tile attachment method
Inconel 718	1600	1310	39	655	Brazed
Ta–10W	700	2020	432	1010	Brazed
Mo (TZM)	760	1400	1098	700	Brazed
Cu (C17510)	1000	1516	1880	758	Brazed
Inconel 718	~0	1310	39	655	Mechanical

[a]Two × yield stress (secondary stress).
[b]Yield stress (primary stress).